Mechanical Systems and Signal Processing 23 (2009) 2019–2028

Contents lists available at ScienceDirect

Mechanical Systems and Signal Processing

journal homepage: www.elsevier.com/locate/jnlabr/ymssp

Time-dependent identification of a bridge-like structure with crossing loads

S. Marchesiello [b,*], S. Bedaoui [a,c], L. Garibaldi [a,b], P. Argoul [a]

[a] Université Paris-Est, UR Navier, Ecole des Ponts ParisTech, 6 & 8 Avenue Blaise Pascal, Champs-sur-Marne, F-77455 Marne-la-Vallée, France
[b] Politecnico di Torino, Dipartimento di Meccanica, Corso Duca degli Abruzzi, 24, I-10129 Torino, Italy
[c] Université M'hamed Bougara, FSI, DGC, Avenue de l'Indépendance, 35000 Boumerdès, Algérie

ARTICLE INFO

Article history:
Received 9 April 2008
Received in revised form
22 December 2008
Accepted 13 January 2009
Available online 31 January 2009

Keywords:
Non-stationary systems
Time-varying systems

ABSTRACT

Time-variant systems must be treated with those algorithms that can take into account the variation of the system with time. In this article, we consider the case of a slender pinned–pinned plate carrying a moving load, simulating the well-known example of a bridge crossed by vehicles or trains.

We propose two different methods to extract dynamic parameters from such a system. The identification is evidently more complex because the system input is unknown (output-only measures).

To simulate such a system and to control the system parameters, a scaled train bridge excited by a crossing train has been built keeping with realistic conditions.

The model described is very useful because of its simplicity and the repeatability of measurements; the goal of this article is to look at the different information given by two alternative tools, developed by two main groups involved in the research.

This system is "almost" linear and it varies with time. In addition, its dynamic parameters change due to the varying position of the load, crossing the system at constant speed. Accelerations are measured along the beam, at different locations.

One of the two methods proposed is a time–frequency approach (CWT) and the other is a modified version of the SSI method, referred to here as short-time stochastic subspace identification (ST-SSI).

Time–frequency maps allow one to follow the instantaneous frequency variations along the bridge crossing and, by adopting the appropriate techniques, these instruments can follow the frequency skeleton and the damping along time, as for the case of the proposed ST-SSI method.

1. Introduction

Non stationarity is supposed to be a signal characteristic, and can be experienced when the statistical properties of the signal are varying along time. Fassois and Poulimenos define by extension, in [1] a "non-stationary system" as a time-varying system that, under random stationary input, gives non-stationary output. Bearing in mind the inherent difficulty in determining whether or not the input force is stationary for a train crossing a bridge, i.e. the excitation given by the rough contact between the wheels and the rails, it is clear that the output can be considered as a non-stationary signal. The main

* Corresponding author.
E-mail addresses: stefano.marchesiello@polito.it (S. Marchesiello), bedaoui@umbb.dz (S. Bedaoui), luigi.garibaldi@polito.it (L. Garibaldi), argoul@lami.enpc.fr (P. Argoul).

0888-3270/$ - see front matter © 2009 Elsevier Ltd. All rights reserved.
doi:10.1016/j.ymssp.2009.01.010

reason is that the mass of the train is non negligible with respect to that of the bridge, and thus the identified modal frequencies of the whole structure are time-varying.

For such a system, special identification tools must be developed and tested using numerically generated time histories or fully controlled lab tests. The system investigated is a scale model of a train crossing a bridge, and originates non-stationary signals in this manner. In fact, since the overall system parameters are time-varying during the different crossing phases, due to the partial or full presence of the train on the bridge, one can experience different statistical characteristics of the signals.

Using time-frequency tools, which are non-parametric methods for processing responses of non-linear or non-stationary systems (see [2]), one can easily detect frequencies holding maximum energy (not necessary eigenvalues), and their variations as a function of the mass (train) position on the bridge deck, as well as damping variations by further elaboration of the signal. In this article, despite the number of tests done on the system, just two examples of single passage are observed in detail and analysed, the final scope being the comparison of two different methodologies.

Together with the cited time-frequency technique, another linear approach derived from the stochastic subspace identification (SSI) method is adopted, and is here referred to as the short-time SSI (ST-SSI) approach; this has been demonstrated to be necessary after testing the classic SSI method (see [3]).

Some results on the railway bridge scaled model highlight the differences between the approaches and clearly indicate the inherent problems of this type of time-variant system, which requires a time-dependent parameter extraction.

2. The state-space model

A linear time-invariant system can be described by a continuous state-space model [4]

$$\begin{aligned} \dot{x} &= A_c x + B_c u \\ y &= Cx + Du \end{aligned} \tag{1}$$

where the output $y(t)$ is a q-dimensional column vector, t is time, the input $u(t)$ is a m-dimensional column vector and the order of the system, i.e. the dimension of the state vector $x(t)$, is n.

The continuous model can be converted into a discrete state-space model assuming zero-order hold for the input u. The discrete state vector is defined as $x_r = x(r\Delta t)$, Δt being the sampling period and following discrete model is obtained:

$$\begin{aligned} x_{r+1} &= Ax_r + Bu_r \\ y_r &= Cx_r + Du_r \end{aligned} \tag{2}$$

where

$$A = e^{A_c \Delta t} \in R^{n \times n} \tag{3}$$

is the dynamical system matrix

$$B = (e^{A_c \Delta t} - I)A_c^{-1} B_c R^{n \times m} \tag{4}$$

is the input matrix, which represents the linear transformation by which the inputs influence the next state, $C \in R^{q \times n}$ is the output matrix that describes how the internal state is transferred to the measurements y_r, and $D \in R^{q \times m}$ is the direct feedthrough matrix.

3. Stochastic subspace identification

It is a well-established technique, and just the reference books by Ljung [5] and by van Overschee and De Moor [6] are here cited, being two milestones fully explicating the theory under this method. Subspace methods take advantage of robust numerical techniques such as QR factorisation and singular value decomposition (SVD) by using geometric tools such as the oblique projections of the row space of matrices.

Given a deterministic-stochastic state-space model with s measurements of the input and of the output:

$$\begin{aligned} x_{r+1} &= Ax_r + Bu_r + w_r \\ y_r &= Cx_r + Du_r + v_r \end{aligned} \tag{5}$$

where w_r and v_r are unmeasurable vector signals called process error and measurement error, respectively, the subspace identification problem consists in estimating the model order n and the system matrices A, B, C and D up to within a similarity transformation. In the "data-driven approach" adopted for this modified version, block Hankel matrices are built up from input and output rough data.

It is worth noticing that the state-space matrices in Eq. (5) can be obtained only within a similarity transformation that is function of the user-defined weighting matrices. So there exists an invertible matrix T such that

$$\begin{aligned} A &= T\hat{A}T^{-1}, \quad B = T\hat{B} \\ C &= \hat{C}T^{-1}, \quad D = \hat{D} \end{aligned} \tag{6}$$

(the symbol ^ denotes estimated matrices). In practice, it is not necessary to compute the matrix T (depending on the choice of the subspace algorithm), because system parameters may be obtained from some matrices, that are invariant under the similarity transformation.

3.1. Short-time SSI

One of the main advantages of the data-driven version of the SSI method, with respect to the covariance-driven approach, is that the former needs a limited number of samples to obtain accurate results.

For this reason, the SSI method can be used to analyse non-stationary systems that are regarded as time-invariant in each user-defined short time-interval, provided they change "slowly" with time. The term "slowly" here mainly means that their time variations are by far longer than their dynamics, i.e. the frequency ranges are well apart.

The covariance-driven approach [7], on the other hand, requires long data histories to be acquired and to build up the Hankel matrix; by using this alternative approach, in fact, the effect is an average of the responses over the time, resulting in global averaged values of parameters and hence losing the instantaneous content.

A similar piece-time approach is adopted for example in [8], to derive a new method for predicting time-varying stochastic systems.

To tune the ST-SSI method, however, some of the parameters must be selected accordingly to treat the data; the key parameters of the "Short-Time SSI" are:

- l (number of columns in block Hankel matrices),
- i (number of block rows of the observability matrix),
- n (model order),
- $2i+l-1$ (window length), and
- m (forward step in the overlapping segment case).

A balance among these parameters must be achieved to obtain a sufficient time resolution, while maintaining the reliability of the results.

4. Instantaneous indicators based on continuous wavelet transform

To better understand non-stationary signals, three instantaneous real indicators based on the wavelet analysis of modulated amplitude and frequency signals [2], are then proposed. These indicators are deduced from the computation of the CWT $W_y(b, a)$ of the studied signal $y(t)$ of finite energy

$$W_y(b,a) = \frac{1}{a}\int_{-\infty}^{+\infty} y(t)\psi^*\left(\frac{t-b}{a}\right) dt$$

where $\psi(t)$ is an analysing function called mother wavelet and $\psi^*(t)$ its complex conjugate.

They are dependent on time b and defined by

$$I_1(b) = \frac{1}{2\pi}\frac{\omega_0}{a_r(b)}, \quad I_2(b) = \ln\left|\frac{W_y(b,a_r(b))}{2\Psi(\omega_0)}\right|,$$
$$I_3(b) = \frac{1}{W_y(b,a_r(b))}\frac{d(W_y(b,a_r(b)))}{db} \tag{7}$$

where

- $a_r(b)$ is a smooth and slow varying curve in the time-scale plane called "ridge". When the energetic representation is based on the absolute value of the CWT: $|W_y(b, a)|$, $a_r(b)$ is defined as the curve where $|W_y(b, a)|$ is maximum. The energy tends to "localize" around the ridge $a_r(b)$, which can be then extracted from $|W_y(b, a)|$,
- $|W_y(b, a_r(b))|$ is the absolute value of the CWT along the ridge. It is called the skeleton.
- ω_0 is the angular frequency where $|\Psi(\omega)|$ is maximum, $\Psi(\omega)$ being the Fourier transform of the mother wavelet $\psi(t)$: $\Psi(\omega) = \int_{-\infty}^{+\infty} y(t)e^{i\omega t}dt$, where $i = \sqrt{-1}$.

The indicator $I_1(b)$ has the dimension of a frequency and $I_2(b)$, $I_3(b)$ characterize the energy and the variation of the energy of the skeleton, respectively.

Let us now examine the expressions of the three previous indicators when the signal $y(t)$ can be expressed as a sum of N chirps $y_j(t)$

$$y(t) = \sum_{j=1}^{N} y_j(t) = \sum_{j=1}^{N} A^{y_j}(t)\cos\left(\alpha^{y_j}(t)\right) \text{ with } \left|\frac{d\alpha^{y_j}(t)}{dt}\right| \gg \left|\frac{1}{A^{y_j}(t)}\frac{dA^{y_j}(t)}{dt}\right| \tag{8}$$

where $A^{y_j}(t) \geqslant 0$ and $\alpha^{y_j}(t) \in [0, 2\pi)$ for all t real.

Each chirp $y_j(t)$ is a frequency modulated signal in which its phase $\alpha^{y_j}(t)$ varies much more rapidly than its amplitude $A^{y_j}(t)$. They are said to be asymptotic in the sense that they tend asymptotically to an oscillatory signal without amplitude modulation. It can be shown [9–11] that the three indicators defined in Eq. (7) become for the jth ridge

$$I_{1_j}(b) = \frac{1}{2\pi}\frac{d\alpha^{y_j}(b)}{db}, \quad I_{2_j}(b) = \ln|A^{y_j}(b)|, \quad I_{3_j}(b) = \frac{1}{A^{y_j}(b)}\frac{dA^{y_j}(b)}{db} \tag{9}$$

$I_{1_j}(b)$ represents the jth instantaneous frequency.

Finally, in the particular case of free accelerometric responses $y_k(t)$ of discrete linear mechanical systems at point k, Eq. (9) can be rewritten

$$I_{1_j}(b) = \frac{1}{2\pi}\omega_{d_j}, \quad I_{2_j}(b) = -\xi_j\omega_j b + \ln(|G_j||\phi_{kj}|\omega_j^2), \quad I_{3_j}(b) = -\xi_j\omega_j \tag{10}$$

where $\omega_{d_j} = \omega_j\sqrt{1-\xi_j^2}$, ω_j and ξ_j being the angular frequency for the conservative underlying system and the modal damping ratio, respectively, for the jth mode, G_j is a constant complex number depending on both the mass and damping

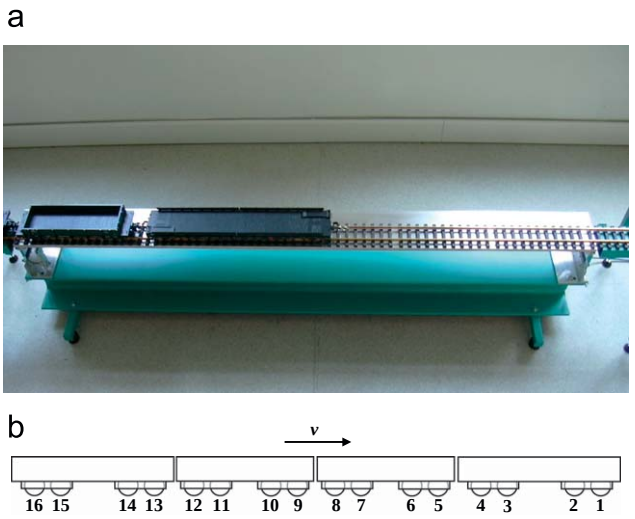

Fig. 1. Photo of the system used for the experimental tests and the train, which is composed by four wagons, of two different lengths.

Table 1
Model scale factors.

	Real bridge	Model	Scale factor
Length (m)	40	1.86	$K_x = 46.5 \times 10^{-3}$
Mass (kg)	2275×10^3	12.48	$K_m = 5.486 \times 10^{-6}$

Table 2
Bridge-like model properties.

Length l (mm)	Width b (mm)	Thickness s (mm)	Young's modulus E (N/m^2)	Density ρ (kg/m^3)	Plate mass m' (kg)	Ballast mass m'' (kg)	Total mass m (kg)
1860	150	15	7×10^{10}	2700	11.3	1.18	12.48

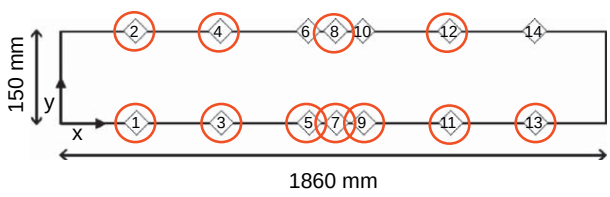

Fig. 2. Measurement points (circles denote the selected points).

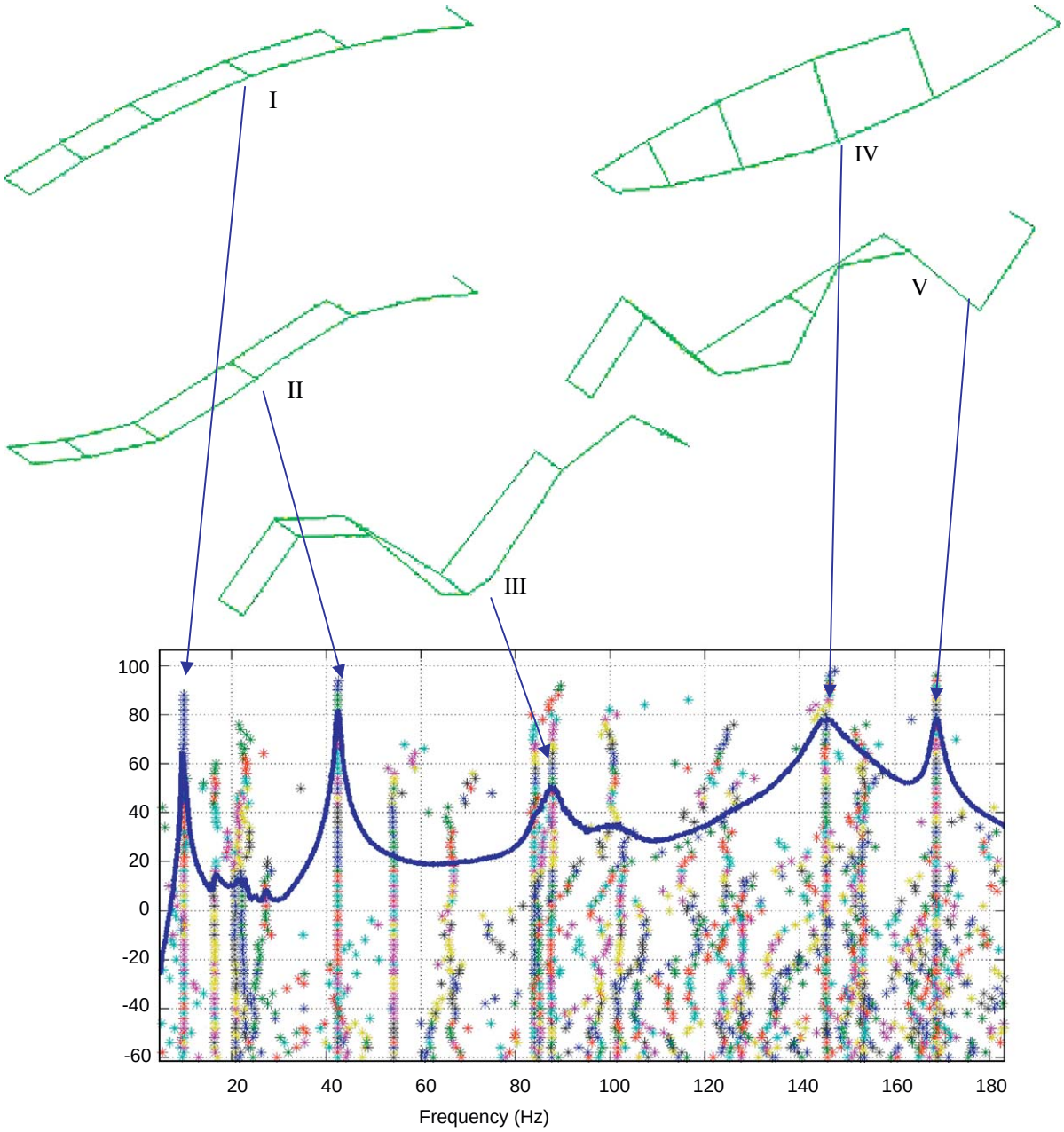

Fig. 3. First five mode shapes of the bridge, obtained by means of SSI.

Table 3
SSI analysis on the bridge alone.

	Mode I	Mode II	Mode III	Mode IV	Mode V
Frequency (Hz)	9.98	42.52	87.58	145.61	168.82
Damping (%)	1.7	1.0	2.3	2.3	0.60

matrices, the jth eigenvector ϕ_j and the initial conditions in displacement and velocity, ϕ_{kj} is the kth component of the complex eigenvector ϕ_j (see [11] for more details).

The resolution of the CWT is a relevant criterion for its use in detection and characterization of non-stationary or non-linear systems. To characterize the mother wavelet resolution, the authors [10,11] introduced the Q-factor defined as the

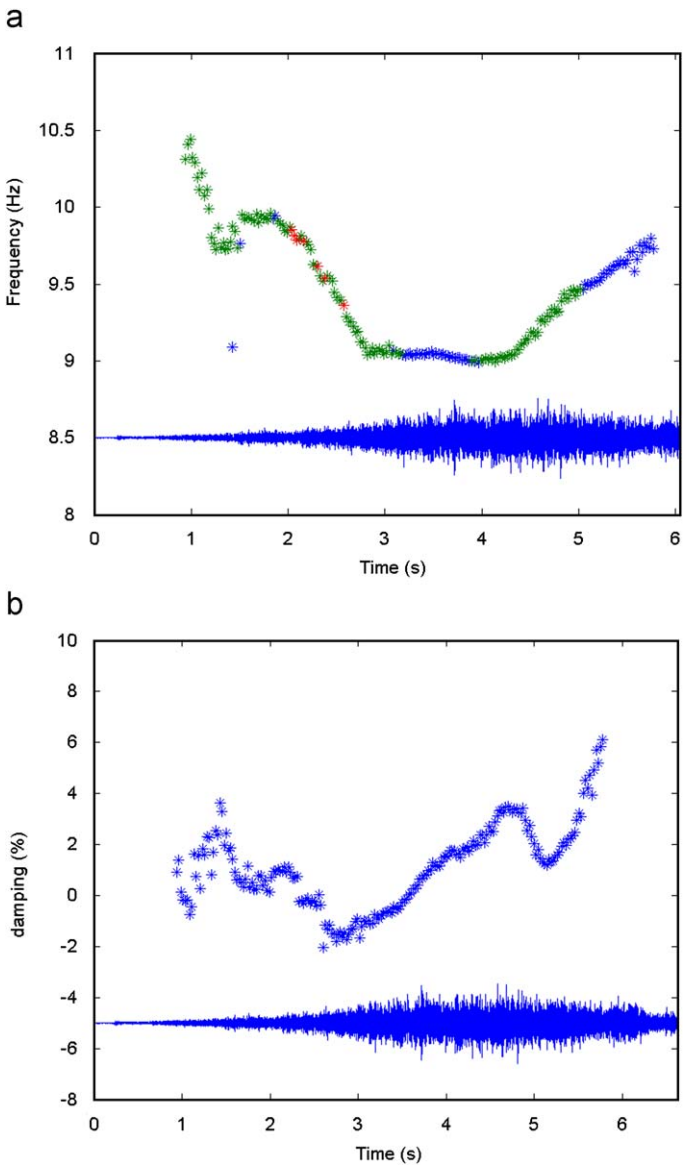

Fig. 4. Frequency (a) and damping (b) evolution, estimated by the ST-SSI (the time histories are superimposed to clarify data interpretation).

ratio between the centre-frequency and the frequency bandwidth of the mother wavelet. More precisely, in [11], three reference values of Q are proposed to remedy edge effects problem and modal coupling, namely: Q_{min}, Q_{max} and Q_ξ. Their expressions are, respectively: $Q_{min} = 5\omega_j/2d\omega_j$, $Q_{max} = \omega_j L/10$ and $Q_\xi \approx 1/\sqrt{2}\xi$ where: L is the length of $y(t)$, ω_j is the studied frequency, $d\omega_j$ is a characteristic discrepancy between two close frequencies. The inequality $Q_{min} < Q_{max}$ must always hold and two cases are distinguished: (a) if $Q_{min} < Q_\xi$ then $Q = \min(Q_\xi, (Q_{min}+Q_{max})/2)$ and (b) if $Q_{min} \geqslant Q_\xi$ then $Q = Q_{min}$.

In this study, we use the Cauchy's mother wavelet: $\psi(t) = (i/t+i)^{n+1}$ which is admissible and progressive [10]. We have: $Q = \sqrt{2n+1}/2$, $\omega_0 = n$, its Fourier transform is:$\Psi(\omega) = (2\pi/n!)\omega^n e^{-\omega}\Theta(\omega)$, where $\Theta(\omega)$ is the unit step function and $\Psi(\omega_0) = 2\pi(n^n/n!)e^{-n}$.

The proposed procedure to analyse the signal $y(t)$ can be performed into six steps: (1) choose the frequency bandwidth around the frequency under study, (2) compute Q_{min}, Q_{max} and Q_ξ and deduce the value of the Q-factor, (3) calculate numerically the CWT of $y(t)$ by means of fast Fourier algorithms: $W_y(b, a) = (1/2\pi)\int_{-\infty}^{+\infty} Y(\omega)\Psi^*(a\omega)e^{i\omega b}db$, (4) extract the ridge by the crazy climber algorithm (for more details see [9] and [10]), (5) calculate the three indicators defined in Eq. (7); for the numerical computation of the derivative: $d(W_y(b, a_r(b)))/db$; a smoothing procedure of the skeleton curve is made

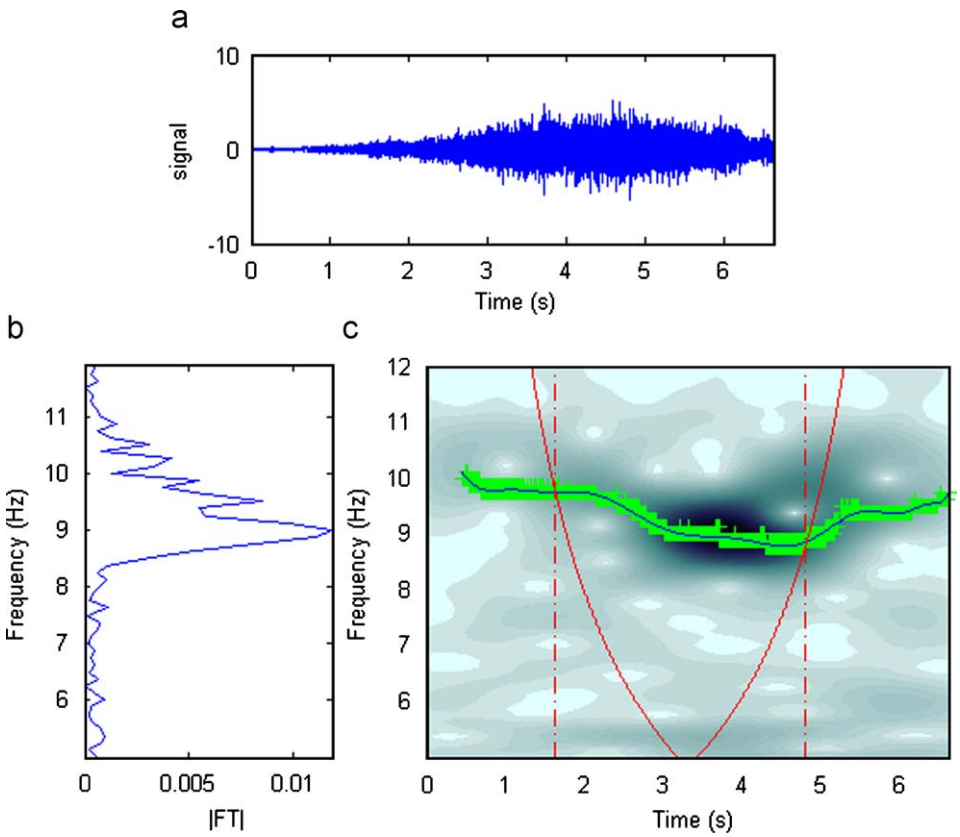

Fig. 5. Experimental signal: energetic representation with dominant energy frequency and the ridges determined by the "Crazy Climbers" algorithm: (a) signal, (b) Fourier spectrum, and (c) scalogramme with ridge evolution ($Q = 20$ and frequency target $f_j = 9\,\text{Hz}$).

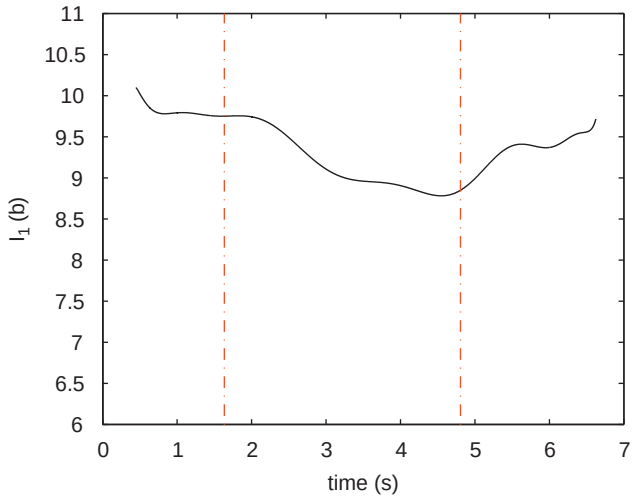

Fig. 6. I_1 indicator evolution over the time.

through the use of an interpolation of the skeleton curve by spline functions, and finally (6) compute a new coefficient expressed as $|I_{3_j}(b)|/I_{1_j}(b)\sqrt{4\pi^2 + (I_{3_j}(b)/I_{1_j}(b))^2}$, which represents an equivalent viscous damping ratio, characterizing the variation of energy during the test (increasing or decreasing energy). In the case of free responses of linear systems, it allows to estimate the jth damping factor ξ_j. The condition for the asymptoticity of $y_j(t)$ can be checked by $2\pi|I_{1_j}(b)| \gg |I_{3_j}(b)|$.

5. The experimental bridge-like rig and the results

The experimental set-up shown in Fig. 1 was designed with particular care, especially regarding the boundary conditions, to realize a pinned–pinned like condition and the dimensional coherence between the bridge and the train. In fact, the parameter choice involved the length, which is responsible for the spatial force distribution, the mass, on which the intensity of the force transmitted depends, as well as the velocity, which is responsible for the spectrum of the input.

A DC electrical motor pulled the train by a wire (to avoid electrical interferences) at constant velocity. The mass of the train was settled by means of a series of calibrated weights. The other system parameters were selected so as to preserve similarity to a real bridge-train system. The chosen scale factors are summarised in Table 1. The scale factor for the velocity was kept equal to that for the longitudinal dimension of the bridge ($K_v = K_x$), since the scale factor for the time was unity ($K_t = 1$). The other parameters were selected so that the first natural frequency would be at about 10 Hz to avoid coupling motions with the supporting structure. The parameter values are shown in Table 2.

A number of input–output measurements (a single point vertical force and the vertical accelerations of 11 points along the structure, see Fig. 2) were first conducted on the scaled model, to investigate its modal properties by exciting the bridge without the train. Data were recorded by means of a 16 channels acquisition system with sampling frequency equal to 4096 Hz, and a band-limited white-noise input was generated in the frequency range from 2 to 512 Hz and applied by an electrodynamic shaker. Results of this stationary analysis (the bridge alone) by means of the SSI data-driven approach [6] are reported in Fig. 3, where the first five identified mode shapes are shown, together with the stabilization diagram and

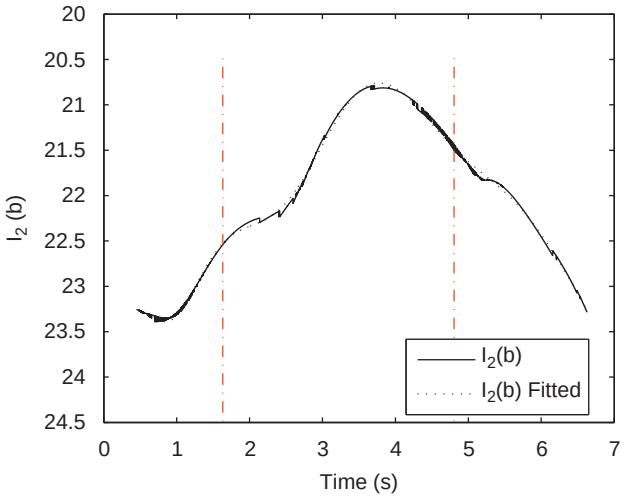

Fig. 7. I_2 indicator evolution over the time.

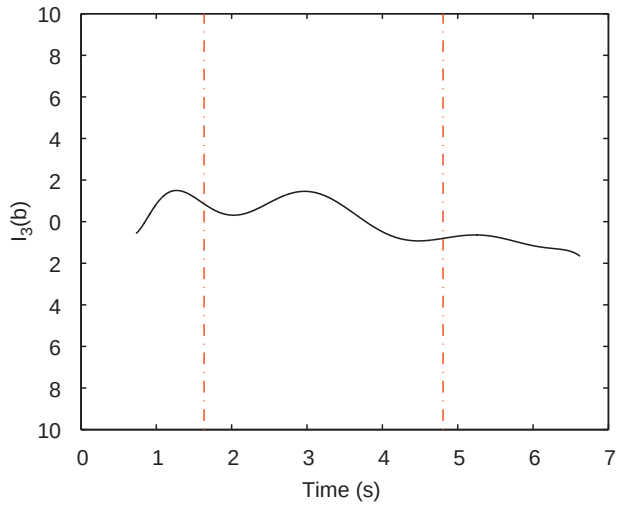

Fig. 8. I_3 indicator evolution over the time.

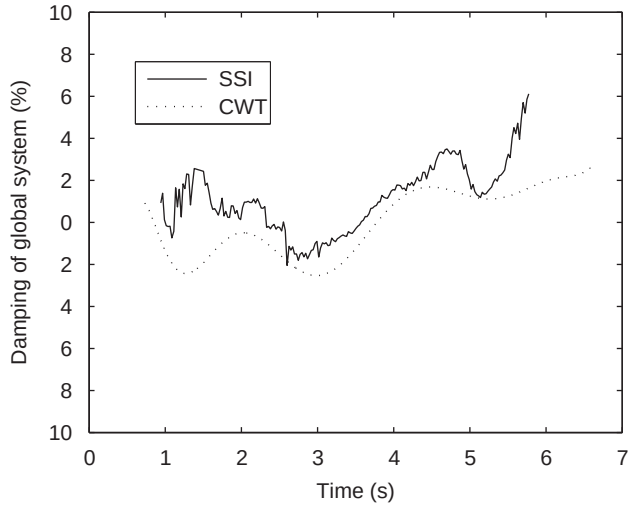

Fig. 9. Comparison between damping estimation of ST-SSI and CWT methods.

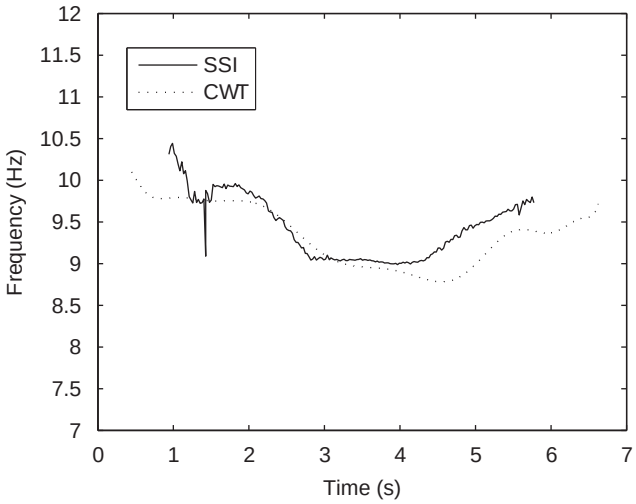

Fig. 10. Comparison between frequency estimation of ST-SSI and CWT methods.

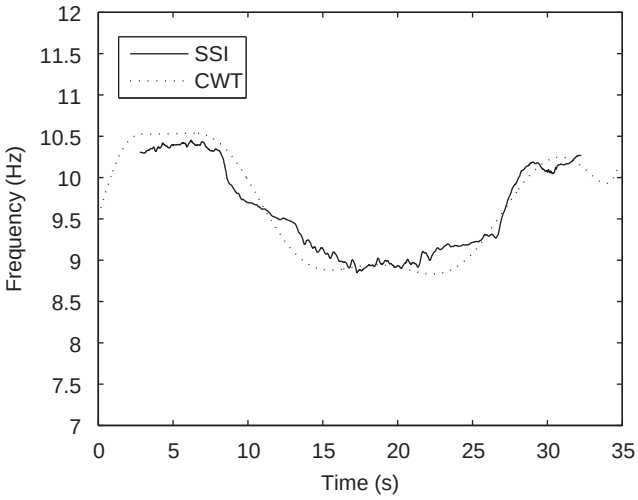

Fig. 11. Comparison between frequency estimation of ST-SSI and CWT methods. Second case: slower train passage.

the sum of the absolute values of the inertances associated to the 11 measurement points. The first five identified modal frequencies and dampings are reported in Table 3. The FRF in Fig. 3 also shows some secondary peaks corresponding to the suspension modes of the whole structure including the I-shaped beam, on which the aluminum plate is mounted (see Fig. 1).

Results of the non-stationary analysis with sampling frequency of 4096 Hz and speed of 0.5 m/s approximately, limited to the first mode shape between 9 and 10 Hz, are reported in Fig. 4 for the analysis by means of the ST-SSI data-driven approach and in Figs. 5–8 for the analysis performed by means of the CWT method. The structure is only excited by the travelling train, since no shaker was used in that case.

Figs. 9 and 10 show the comparison of the frequency and damping evolution extracted by the two different methods.

A second case is then considered with train speed six times lower than that of previous figures, while the load remains unchanged. In Fig. 11, the first modal frequency evolutions extracted by the two methods are compared.

6. Comments and conclusions

Although the two methods use fully different approaches, the results obtained seem to be reasonably comparable. The ST-SSI method seems slightly noisier in terms of frequency and damping extracted, as for the case of a negative peak extracted in frequency estimation at around 1.5 s (Fig. 10), which is probably due to a computational mode.

Also for the same case, the initial part of the extracted values is noisier for both frequency and damping: this is probably caused by the lower excitation level (and hence lower signal and worse S/N ratio) during the train approaching and the initial part of its crossing. It is also interesting to notice that both methods identify negative damping values in the first part of the time history. In this phase, the structure, which is initially at rest (or more precisely, lightly excited due to vibration transmission along the rail), starts to be directly loaded by the train and strongly excited by it; the vibration amplitude of the bridge, particularly the amplitude of the first mode under analysis, is dramatically increasing. This is the meaning of the negative apparent damping during this phase.

From Fig. 11, where the frequency evolution for a slower train passage is depicted, it is clear that CWT may suffer from edge effects and this may be considered as a drawback of this method compared to ST-SSI.

One of the main differences between the methods is in the global sense of the extracted parameter: whilst the CWT method is analysing one sensor record at each time, the ST-SSI allows the contemporary analysis of all time histories from the sensors, at the same time, hence giving a "global" value of the extracted parameters. In [12], Le and Paultre processed conjointly several responses of structures under ambient excitations by using CWT and correlation function; the redundant information being removed using singular value decomposition.

The evolutionary parameters constitute a powerful information to verify the system symmetry, and hence the presence of structure defects, but they are also fundamental to extract information on the relationship among the load transit characteristics (weight, speed and so on) and the extracted parameters.

The latter type of analysis allows a deeper investigation for diagnostics and monitoring purposes, which are out of scope of this paper, and whose fundaments lie in a robust and reliable analysis of time-varying parameters.

References

[1] A.G. Poulimenos, S.D. Fassois, Parametric time-domain methods for non-stationary random vibration modelling and analysis—a critical survey and comparison, Mechanical Systems and Signal Processing 20 (4) (2006) 763–816.
[2] P. Argoul, T.-P. Le, Instantaneous indicators of structural behaviour based on the continuous Cauchy wavelet analysis, Mechanical Systems and Signal Processing 17 (1) (2003) 243–250.
[3] L. Garibaldi, S. Marchesiello, Non stationary analysis of a railway bridge scaled model under operational conditions, in: Proceedings of the ISMA2006 Conference, Leuven, Belgium 2006, September 18–20.
[4] S. Marchesiello, L. Garibaldi, A time domain approach for identifying nonlinear vibrating structures by subspace methods, Mechanical Systems and Signal Processing 22 (1) (2008) 81–101.
[5] L. Ljung, System Identification: Theory for the User, second ed., Prentice-Hall, Upper Saddle River, NJ, USA, 1999.
[6] P. van Overschee, B. De Moor, Subspace Identification for Linear Systems: Theory–implementation–applications, Kluwer Academic Publishers, Dordrecht, The Netherlands, 1996.
[7] L. Garibaldi, S. Marchesiello, E. Bonisoli, Identification and up-dating over the Z24 benchmark, Mechanical Systems and Signal Processing 17 (1) (2003) 153–161.
[8] K. Kameyama, A. Ohsumi, Subspace-based prediction of linear time-varying stochastic systems, Automatica 43 (12) (2007) 2009–2021.
[9] R. Carmona, W.-H. Hwang, B. Torrésani, Practical time–frequency analysis, Academic Press, New York, 1998.
[10] T.-P. Le, P. Argoul, Continuous wavelet transform for modal identification using free decay, Journal of Sound and Vibration 277 (1–2) (2004) 73–100.
[11] S. Erlicher, P. Argoul, Modal identification of linear non-proportionally damped systems by wavelet transform, Mechanical Systems and Signal Processing 21 (3) (2007) 1386–1421.
[12] T.-P. Le, P. Paultre, Time–frequency domain decomposition for modal identification using ambient excitation tests, in: Proceedings of the ISMA2006 Conference, Leuven, Belgium 2006, September 18–20.